ORIENTAL JOURNAL OF CHEMISTRY
An International Open Access, Peer Reviewed Research Journal
www.orientjchem.org
ISSN: 0970-020 X
CODEN: OJCHEG
2024, Vol. 40, No.(2):
Pg. 604-610

Effect of Al_2O_3 Nanoparticle on the characteristic Parameters of PVDF-co-HFP Based Mg^{2+} Conducting Polymer Electrolyte Membranes

M. RAM REDDY[1,2]*, RAMBABU GUNDLA[2], V. MADHUSUDHANA REDDY[3] and N. KUNDANA[1]

[1]B. V. Raju Institute of Technology, Narsapur, Medak, India.
[2]Department of Chemistry, School of Technology, GITAM University, Hyderabad, India.
[3]MallaReddy College of Engineering and Technology, Hyderabad, India.
*Corresponding author E-mail: kundananakkala@gmail.com

http://dx.doi.org/10.13005/ojc/400237

(Received: January 13, 2024; Accepted: March 15, 2024)

ABSTRACT

Solution casting technique was cast-off to create a novel kind of magnesium ion conductive nanocomposite polymer electrolyte membrane. The films include dissimilar weight percentages of Al_2O_3 nanofillers embedded in the congregation polymer PVDF-co-HFP, containing magnesium triflate $Mg(CF_3SO_3)_2$. The distinctive crystalline phases of the polymer and its segment dynamics are considerably changed by changes in the component content of these SPEs. The structural morphology of these films were characterized by the techniques such as FTIR, DSC, SEM, and XRD. Fourier transform infrared spectroscopy (FTIR) was used to affirm the chemical composition of the polymer electrolyte membrane, Differential scanning calorimetry (DSC) was used to verify a decline in melting temperature, Scanning electron microscopy (SEM) was used to affirm the exterior morphology of the film, and Xray diffraction (XRD) was used to ensure the drop in crystallinity. It was observed that 8wt% of Al_2O_3 exhibits the best among them. The addition of nano filler was found to trigger the band of C–O–C stretching to move to a lesser wave number and the strength of the peaks to drop, signalling that the films' crystalline nature had changed to an amorphous one.

Keywords: Solution casting method, Nanofiller, DSC, FTIR, SEM and XRD.

INTRODUCTION

Solid-state polymer electrolytes have garnered a lot of attention due to its potential in solid-state electrochemical devices-which span a extensive range of applications, including chemical sensors, fuel cells, super capacitors, and rechargeable batteries[1,2,3,4]. Solid polymer electrolytes (SPEs), as compared to liquid electrolytes, have an array of features. The advantages of this technique include preventing leakage of electrolytes, safe handling, a broad range of operating temperatures, and improved device longevity.[5,6,7] Fabricating devices in the desired shape can be made easier by the flexibility, mold ability, mechanical, thermal, and electrochemical stability of polymer electrolyte thin films. The alkali or alkaline

earth metal salt is dispersed in the host polymer to generate these polymer electrolytes[8,9,10,11,12,13]. Poly ethylene oxide, poly vinyl alcohol, and poly vinylidene fluoride are a few examples of host polymers. However, of all the polymers, PVDF-co-HFP has been studied the most because it contains crystalline vinyl groups (-CH_2-CF_2-) that have the ability to attract ions of ionic salts[14,15]. The magnesium ion that was used in this work is obtained using the ionic salt $Mg(CF_3SO_3)_2$, which is affordable, readily available, easy for handling in an open environment, and has no adverse effects on health[3]. At room temperature, SPE usually has reduced ionic conductivity. Various researchers investigated on nano composite solid polymer electrolytes (NCPEs) in an attempt to solve this issue.[16,17,18,19,20,21,22,23,24,25]

In general, composite polymer electrolytes are made up of two phases: a solid polymer electrolyte in the early stages and an inert filler material in the later stage, such as ZrO_2, CeO_2, Al_2O_3, SiO_2, and TiO_2, among others.[26,27,28,29] Since fillers' dispersion improves polymer electrolytes' mechanical durability, thermal stability, biodegradability, and ionic conductivity. we're looking at the Dispersion of Al2O3 nano-filler in this study. The rise in amorphous nature of the polymer electrolyte, which facilitates fast ion transport and favors ion pair dissociation, as well as segmental movement of the polymer chain, are what's responsible for the upsurge in ionic conductivity. The majority SPE/NCPE films are cast through the solution casting methodology. This method is affordable as well as easy to perform.

Li technology is expensive and highly reactive, which makes it challenging to utilize in an open environment. Therefore, efforts have been made to find alternative options, such as Mg batteries. Magnesium ions, which have an ionic radius of 0.086 nm, are about the same size as lithium ions, which have an ionic radius of 0.090 nm. They are also stable by nature, cheap, and easily accessible. Wu et al. reported on a magnesium-based polymer electrolyte in 2017.

We investigated the impact of Al_2O_3 nano-filler dispersion in the ideal conducting composition of 70 wt%PVDF-30 wt%$Mg(CF_3SO_3)_2$ on the ionic conductivity of Solid Polymer Electrolyte thin films made by solution casting technique. To examine the structural and thermal characteristics of the material, X-ray diffraction (XRD) and Differential scanning calorimetry- (DSC) were performed. -To know there structural morphology FTIR & SEM analysis is done.

EXPERIMENTAL

Chemicals Required

The ingredients used for the synthesis of nanocomposite polymer electrolyte membranes comprises Poly(vinylidene fluoride-co-hexafluoropropylene), average M_w~400,000, the salt Magnesium trifluoromethanesulfonate $Mg(CF_3SO_3)_2$ (MWt=322.4), Nano filler Al_2O_3(~50nm) from sigma aldrich and Tetra hydro furan [THF] solvent are acquisition from Merck. The membrane is made using a technique known as solution casting. 30wt% $Mg(CF_3SO_3)_2$ and 70wt% PVDF-co-HFP were employed in this procedure. As was already said, fervently mix for 48 h at an uninterrupted temperature of 50°C to create an even mixture. To generate a 50 µm-thick nanocomposite polymer electrolyte membrane, a viscous solution containing PVDF-co-HFP/$Mg(CF_3SO_3)_2$/Al_2O_3 was put into a petri dish, and THF was allowed to exit under ambient conditions. Table 1 displays the codes for the four electrolyte samples that were created and made ready.

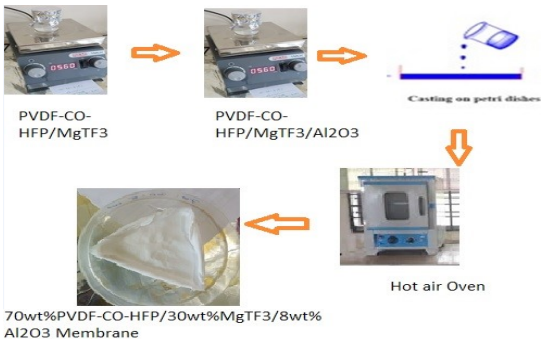

Fig. 1(a). The schematic illustration of Nanocomposite polymer electrolyte membranes

Table1: Composition ratio of Synthesized samples

S. No	Sample code	PVDF-co-HFP(wt%)	$Mg(CF_3SO_3)_2$(wt%)	Al_2O_3(wt%)	THF(wt%)
1	PMA-0	70	30	0	50
2	PMA-4	70	30	4	50
3	PMA-8	70	30	8	50
4	PMA-12	70	30	12	50

Instrumentation

Using an Ultima-IV X-ray diffractometer and a Copper X-ray tube as the radiation source, the X-ray diffraction pattern was captured at 40kV/30mA. Polymer electrolyte membrane SEM micrographs were taken with an FEI Quanta 200 microscope. A 'Shimadzu' 8202 PC "Fourier transform infrared" (FTIR) 'spectrophotometer' with a transmittance range of 2000 to 450 cm^{-1} was used to assess the films' structural and functional efficacy. The differential scanning calorimeter used was a Shimadju DSC-60.

RESULT AND DISCUSSION

X-ray diffraction analysis

XRD results show that Al nanoparticles Successfully encapsulated in PVDF-co-HFP/ $Mg(CF_3SO_3)_2$ membranes. Crystal peaks of Al nanoparticles encapsulated in PVDF-co-HFP/ $Mg(CF_3SO_3)_2$ membrane clearly visible. PVDF-co-HFP/$Mg(CF_3SO_3)_2$ membranes' amorphous nature is only apparent from two peaks before Al nanoparticles are added. The XRD spectral peaks of the PVDF-co-HFP: $Mg(CF_3SO_3)_2$ doped nano composite electrolyte membranes were analyzed. The XRD arrays of all created NCPEMs can be conspired using the Bragg angle 2θ against their respective intensities, as illustrated in Fig. 1. By broadening the XRD peaks, planar PVDF-co-HFP films show the observed semi-crystalline phase at 18, 20.3, 27, and 39 degrees. The crystallization characteristics of the ionic salt are demonstrated by the strong peaks of the $Mg(CF_3SO_3)_2$ salt at the following angles: 17.6, 19.2°, 20.18°, 30.2°, and 32.6°, respectively. when introducing nano-Al nanoparticles into PVDF-co-HFP/$Mg(CF_3SO_3)_2$ membrane, new peak related to presence Al nanoparticles with coordinates 28.44°, 37.71°and 40.73°. Peak intensity declines with increasing Al nanofiller concentration until it is attained by PVDF-co-HFP/$Mg(CF_3SO_3)_2$/Al_2O_3 (8%Al_2O_3), indicating a transition in the film's properties from crystalline to amorphous, which commendation to an escalation in the electrolyte membrane's conductivity. Additionally, the XRD peak's intensity slightly increases with increasing weight percentage, particularly at 12 wt% Al_2O_3, suggesting the restoration of semi-crystalline nature as shown in Figure 1(b).

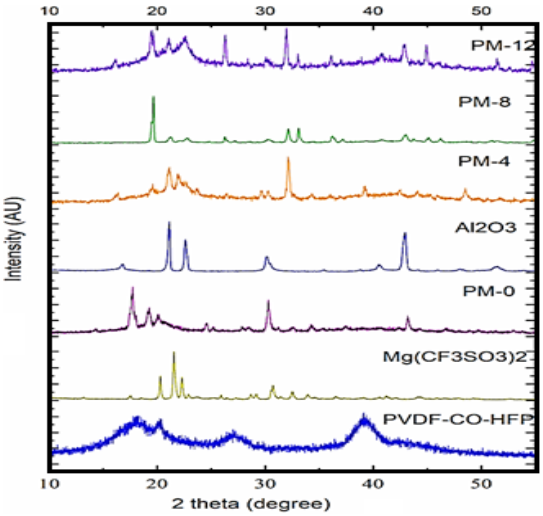

Fig. 1(b). Elaborate The XRD peaks of pure PVDF-co-HFP polymer, $Mg(CF_3SO_3)_2$, are displayed

The polymer electrolytes both with and without nanoparticles at varying weight percentages (i.e., 4, 8, and 12 wt.% Al_2O_3).

FTIR-Spectroscopic Studies

The sample's vibrational modes, functional groups, and bonding characteristics have all been identified via infrared spectroscopy. Additionally, it is utilized to examine interactions between atoms or ions that exist in electrolyte systems. These collaborations encourage alterations to the polymer electrolyte complexation's vibrational modes.

Molecular interactions cause the bands of FTIR absorption peaks to move, broaden, and eventually become extinct when nanofillers are added to polymer salt complexes. Fig. 2 depicts FTIR spectra for each thin membrane with the composition of the electrolyte membrane built of Al_2O_3 @PVDF-co HFP/Mg^{2+}, pure FTIR spectra of PVDF-co-HFP, pure $Mg(CF_3SO_3)_2$ powder and pure Al_2O_3.790 and 1062 cm^{-1} peaks in the crystalline nature of the phase is indicated by the absorption spectra of PVDF-co-HFP, where the α phase is represented by 842 cm^{-1}. (19–21) HFP units have an amorphous phase, whereas PVDF units[22] have a crystalline phase. The Al^{3+} ions' interaction with the PVDF-co-HFP:$Mg(CF_3SO_3)_2$ polymer electrolyte[23] caused the 843 cm^{-1} and 1287 cm^{-1} peaks to dissipate. The reason for these peaks is that PVDF-co-HFP's extended

ferroelectric phase has a reversal order. The peak removal demonstrates that Al^{3+} interacts with the polymer salt host, and the -C-F-rocking at 804 cm^{-1} is expected given the chemical structure of PVDF-co-HFP. Skeletal deformation results from the diminution of the 797 cm^{-1} peak by polymer salt nano complexation. The material is undergoing an alteration. The PVDF-co-HFP polymer's 871 cm^{-1} vibrational peak, which was turned on by CH_2 rocking, has disappeared and a innovative group at 1042 cm^{-1} illustrations that the film is currently in the amorphous segment[24]. The twisting vibration frequency of CH_2 in the membrane structure is represented by the C-C band's 1400 cm^{-1} peak and 1070 cm^{-1} bending vibration. PVDF-co-HFP's peak intensity dropped. Stretching vibration with a C-F symmetry is seen at a second peak at 1280 cm^{-1}. The CF_3 and CF_2 groups' symmetric stretching modes migrate and converge, creating a novel peak at 1230 cm^{-1} and determining its frequency. 1404 cm^{-1} is the shear frequency of CH_2-CF_2. A peak forms at 1545 cm^{-1} and the band at 1402 cm^{-1} vanishes. The deformation of CH_2 is the reason for this new peak. Salts of Al_2O_3 and $Mg(CF_3SO_3)_2$ destroy the peak by decreasing its intensity between 2986 and 3024 cm^{-1}. The absorption peak that was previously assigned has been moved to 3240 cm^{-1} because of the coupling of Mg^{2+} ions to vinylidene -CH_2-CF_2-, which is connected to the host polymer's support. It is thought that the Mg^{2+} ions' effect on HFP stretches the PVDF bonds to ideal values, encouraging the shift from the crystalline to the amorphous phase.[25] The vibration band shifts from 784-813 cm^{-1} to 813-927 cm^{-1} as the concentration drops when PVDF-co-HFP is complexed with $Mg(CF_3SO_3)_2$ salt, signifying the amorphous phase. Al_2O_3 may form between the host polymer and the $Mg(CF_3SO_3)_2$ salt complex when polymer salts are present. When the swarm polymer's observed band frequency changes, some bands vanish and new bands emerge.

The shift and dearth of infrared bands in the pure sample and the new infrared spectra of Al_2O_3-doped polymer composite films show important interactions between PVDF-co-HFP/ $Mg(CF_3SO_3)_2/Al_2O_3$.

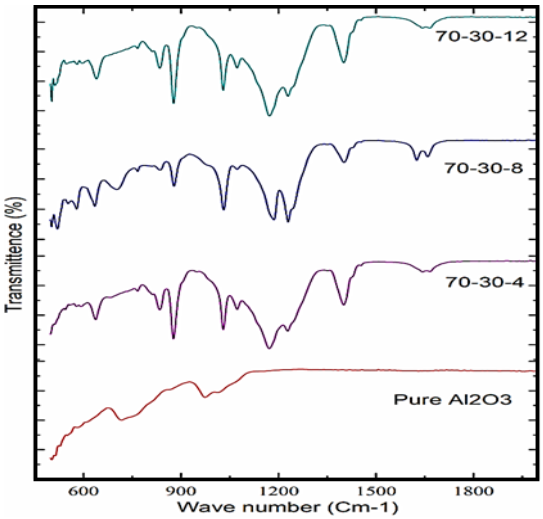

Fig. 2. Elaborate the FTIR Spectra of Unadulterated PVDF-co-HFP Polymer, $Mg(CF_3SO_3)_2$, polymer electrolyte without nano and with different weight percentages of nano i.e, 4, 8, and 12 wt.% of Al_2O_3

SEM analysis

The morphological features of the Nanocomposite films are examined by using Scanning Electron Microscope. Fig. 3 illustrates scanning electron images of pure PVDF-co-HFP, pure $Mg(CF_3SO_3)_2$, and 70wt% PVDF-co-HFP: 30 wt % $Mg(CF_3SO_3)_2$::X wt%Al_2O_3 polymer electrolyte films with x weight percentages of 4, 8, and 12 are shown in figure. The SEM micrographs of the films depicts surface of the film is homogenous. Upon incorporation of Al_2O_3 nanofiller into solid electrolyte films there an increase in surface roughness and decrease in more number of pores. The porosity of the membrane also changes resulting enhancement of mobility of ions. Inside the polymer matrix, a highly porous structure develops as a result of the solvent and polymer's interaction. Consequently, the solvent manages to get out of the polymer layer. The presence of a linked microporous polymer matrix and the inclusion of Al_2O_3 promote the mobility of magnesium ions.[27] The presence and size of pores in the membrane structure increase the mobility of Mg^{+2} ions, which is a positive factor that increases the uptake of the polymer salt electrolyte in the nanocomposite. At the optimal weight percentage of 70:30:8% [PVDF-co-HFP: Al_2O_3: $Mg(CF_3SO_3)_2$]. This phenomenon is illustrated in Fig. 3(a), and the same conclusions are drawn in conjunction with the XRD findings.

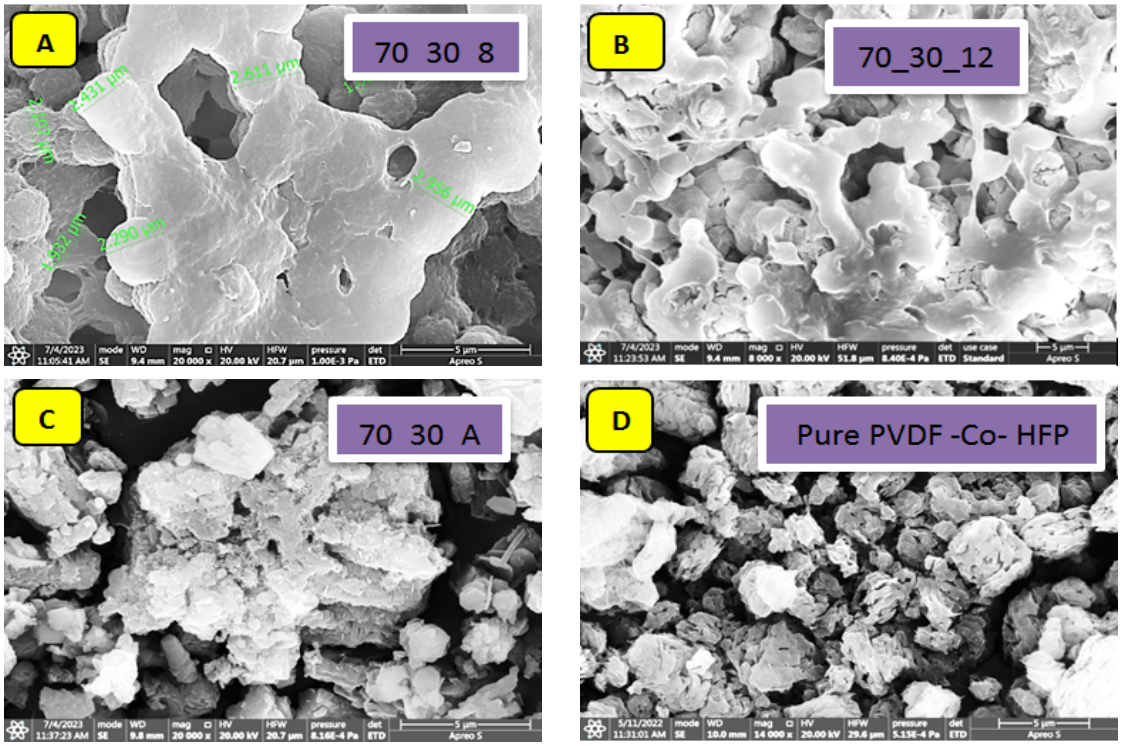

Fig. 3(a). Exemplify the SEM Images of Pure PVDF-co-HFP Polymer, $Mg(CF_3SO_3)_2$, polymer electrolyte without nano and with different weight percentages of nano I.e, 4, 8, and 12 wt.% of Al_2O_3

DSC anaylsis

Utilizing differential scanning colorimetry, the thermal behavior of the membranes is examined. In Fig., the DSC thermograms are displayed The melting point (Tm) and melting point (Tg) of the PVDF-co-HFP copolymer are ±53.04°C and 140.11°C, respectively, according to Fig. 3(b). The glass transition temperature (Tg) and melting point (Tm) of pure magnesium$(CF_3SO_3)_2$ salt are 91.24°C and 133.74°C, respectively. It is observed that the melting temperature of pure polymer PVDF-co-HFP including $Mg(CF_3SO_3)_2$ (PM-0) is 101.5°C. The properties of the film alter when Al_2O_3 is introduced; diffusion peaks show that the semi-crystalline nature is destroyed and complex formation occurs, which is entirely consistent with the findings of the FTIR and XRD analyses. Furthermore, a change in the melting peak towards lower temperatures was observed, suggesting a reduction in the crystallinity of the film. The peak changes toward lower temperatures as the Al_2O_3 concentration rises, offering compelling evidence of rising amorphous content[29]. The maximum shifting and broadening of the peak was noticed for 8wt%Al_2O_3. While at higher concentrations of Al_2O_3, contrary trend is observed and transfer of peak towards higher temperature indicating the enhancement of crystalline nature, depicting decrease of ionic conductivity.

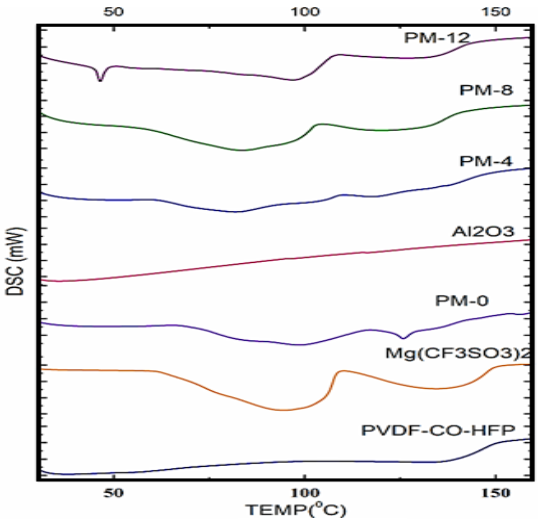

Fig. 3(b). Exemplify the thermograms of Pure PVDF-co-HFP Polymer, $Mg(CF_3SO_3)_2$, polymer electrolyte without nano and with different weight percentages of nano i.e, 4, 8, and 12 wt.% of Al_2O_3

CONCLUSION

Solution casting was used in this study to prepare the Al_2O_3 nanofiller-doped porous structured PVDF-co-HFP:$Mg(CF_3SO_3)_2$ polymer NCPEM. NCPEM has the ability to improve electrical conductivity because of its substantial porosity and amorphous structure, which may prove helpful in the future when creating new kinds of batteries. In order to shrinkage the aperture size and enhance the quantity of apertures in NCPEM, Al_2O_3 nanofillers are added. Employing Al_2O_3 nanofillers as inorganic fillers, the current work successfully decreases the pore size and promotes the amorphous oddity of solid polymer membranes. The phase transition of the prepared PVDF-co-HFP-$Mg(CF_3SO_3)_2$ NCPEM from the semi-crystalline phase to the amorphous phase was verified by FTIR analysis, which also inveterate the chemical interface of $Mg(CF_3SO_3)_2$ with PVDF-co-HFP. SEM analysis reveals the surface shape and porosity characteristics of the right away PVDF-co-HFP-$Mg(CF_3SO_3)$2-Al_2O_3 NCPEM.. XRD reveals that the XRD peak intensity of PVDF-co-HFP:$Mg(CF_3SO_3)_2$ somewhat drops at 8wt% weight percentage of Al_2O_3, suggesting that the semi-crystalline nature is recovered at 12%. There is no amorphous phase left in the Al_2O_3 nanofiller film. Tg and Tm of pure component and salt-doped PVDF-co-HFP:$Mg(CF_3SO_3)_2$ films confirmed by DSC characterization. These findings suggest that when electrolytes and electrodes are added to the PVDF-co-HFP:$Mg(CF_3SO_3)_2$ membrane, inorganic nanofiller particles can increase the membrane's porosity, ion mobility, and stability.

ACKNOWLEDGEMENT

All authors would like to express their gratefulness to the staff members of the Polymer electrolyte Research Laboratory at the Physics Department, the BVRIT Narsapur and GITAM Hyderabad for providing the facilitates for this work

Conflict of interest

The authors further declare that they have no pertinent personal or business interests to disclose, nor do they have slightly conflicting benefits to declare with regard to the contents of this article.

REFERENCES

1. Castro-Gutiérrez, J.; Celzard, A., & Fierro, V. Energy storage in supercapacitors: Focus on tannin-derived carbon electrodes. *Frontiers in materials*., **2020**, *7*, 217.
2. Majumdar, D.; Mandal, M., & Bhattacharya, S. K. Journey from supercapacitors to supercapatteries: recent advancements in electrochemical energy storage systems. *Emergent Materials*., **2020**, *3*, 347-367.
3. Xiao, J.; Anderson, C.; Cao, X.; Chang, H. J.; Feng, R.; Huang, Q., & Sivakumar, B. Perspective—Electrochemistry in understanding and designing electrochemical energy storage systems., *Journal of the Electrochemical Society*., **2022**, *169*(1), 010524.
4. Baumann, A. E.; Burns, D. A.; Liu, B., & Thoi, V. S. Metal-organic framework functionalization and design strategies for advanced electrochemical energy storage devices. *Communications Chemistry*., **2019**, *2*(1), 86.
5. Navarro-Suárez, A. M., & Shaffer, M. S. Designing structural electrochemical energy storage systems: a perspective on the role of device chemistry., *Frontiers in Chemistry*., **2022**, *9*, 810781.
6. Kundana, N.; Venkatapathy, M.; Neeraja, V.; Espenti, C. S., & Reddy, V. M. Preparation and characterization of solid polymer electrolyte membranes based on pvdf-co-hfp polymer and mgtf3 as a dopant., *Rasayan Journal of Chemistry*., **2022**, *15*(4), 2359-2365.
7. Aurbach, D.; Markevich, E., & Salitra, G. High energy density rechargeable batteries based on Li metal anodes. The role of unique surface chemistry developed in solutions containing fluorinated organic co-solvents., *Journal of the American Chemical Society*., **2021**, *143*(50), 21161-21176.
8. Yuan, X.; Ma, F.; Zuo, L.; Wang, J.; Yu, N.; Chen, Y., & van Ree, T. Latest advances in high-voltage and high-energy-density aqueous rechargeable batteries., *Electrochemical Energy Reviews*., **2021**, *4*, 1-34.
9. Yuan, X.; Wu, X.; Zeng, X. X.; Wang, F.; Wang, J.; Zhu, Y., & Duan, X. A fully aqueous hybrid electrolyte rechargeable battery with high voltage and high energy density., *Advanced Energy Materials*., **2020**, *10*(40), 2001583.

10. Durmus, Y. E.; Zhang, H.; Baakes, F.; Desmaizieres, G.; Hayun, H.; Yang, L., & Eind Eli, Y. Side by side battery technologies with lithiumion based batteries., *Advanced Energy Materials*., **2020**, *10*(24), 2000089.
11. Xie, Y.; Gabriel, E.; Fan, L.; Hwang, I.; Li, X.; Zhu, H., & Xiong, H. Role of lithium doping in P2-Na0. 67Ni0. 33Mn0. 67O2 for sodium-ion batteries. *Chemistry of Materials.,* **2021**, *33*(12), 4445-4455.
12. Tarascon, J. M. Key challenges in future Li-battery research. Philosophical Transactions of the Royal Society A: Mathematical, Physical *and Engineering Sciences*., **2010**, *368*(1923), 3227-3241.
13. Jiang, M.; Mu, P.; Zhang, H.; Dong, T.; Tang, B.; Qiu, H., & Cui, G. An endotenon sheath-inspired double-network binder enables superior cycling performance of silicon electrodes. *Nano-Micro Letters*., **2022**, *14*(1), 87.
15. Alipoori, S.; Mazinani, S.; Aboutalebi, S. H.; & Sharif, F. Review of PVA-based gel polymer electrolytes in flexible solid-state supercapacitors: Opportunities and challenges. *Journal of Energy Storage*., **2020**, *27*, 101072.
16. Elkalashy, S.; Gamal, R.; Sheha, E., & El Kholy, M. M. Polymer Electrolytes Based on Magnesium Triflate for Quasi-Solid-State Magnesium-Sulfur Batteries. Available at SSRN 4020121.
17. Tripathi, M.; Bobade, S. M., & Kumar, A. Preparation of polyvinylidene fluoride-co-hexafluoropropylene-based polymer gel electrolyte and its performance evaluation for application in EDLCs., *Bulletin of Materials Science*., **2019**, *42*, 1-10.
18. Singh, V. K., & Singh, R. K. Development of ion conducting polymer gel electrolyte membranes based on polymer PVdF-HFP, BMIMTFSI ionic liquid and the Li-salt with improved electrical, thermal and structural properties., *Journal of Materials Chemistry C*., **2015**, *3*(28), 7305-7318.
19. Ulaganathan, M., & Rajendran, S. Effect of different salts on PVAc/PVdF co HFP based polymer blend electrolytes., *Journal of Applied Polymer Science*., **2010**, *118*(2), 646-651.
20. Janakiraman, S.; Agrawal, A.; Biswal, R., & Venimadhav, A. An amorphous polyvinylidene fluoride-co-hexafluoropropylene based gel polymer electrolyte for sodium-ion cells. *Applied Surface Science Advances*., **2021**, *6*, 100139.
21. Prabakaran, K.; Mohanty, S., & Nayak, S. K. Improved electrochemical and photovoltaic performance of dye sensitized solar cells based on PEO/PVDF–HFP/silane modified TiO_2 electrolytes and MWCNT/Nafion® counter electrode., RSC Advances., **2015**. *5*(51), 40491-40504.
22. Ruan, L.; Yao, X.; Chang, Y.; Zhou, L.; Qin, G., & Zhang, X. Properties and applications of the α phase poly (vinylidene fluoride)., *Polymers*., **2018**, *10*(3), 228.
23. Abbrent, S.; Plestil, J.; Hlavata, D.; Lindgren, J.; Tegenfeldt, J., & Wendsjö, Å. Crystallinity and morphology of PVdF–HFP-based gel electrolytes., *Polymer*., **2001**, *42*(4), 1407-1416.
24. Wang, T. H.; Wang, W. X., & Chang, H. C. Pressure-dependent clustering in ionic-liquid-poly (vinylidene fluoride) mixtures: an infrared spectroscopic study., *Nanomaterials*., **2021**, *11*(8), 2099.
25. Xia, W., & Zhang, Z. PVDF-based dielectric polymers and their applications in electronic materials., *Iet Nanodielectrics*., **2018**, *1*(1), 17-31.
26. Fortunato, M.; Cavallini , D.; De Bellis, G.; Marra, F.; Tamburrano, A.; Sarto, F., & Sarto, M. S. Phase inversion in PVDF films with enhanced piezoresponse through spin-coating and quenching., *Polymers*., **2019**, *11*(7), 1096.
27. Lin, Z.; Wu, J.; Qiao, W.; Zhao, Y.; Wong, K. H.; Chu, P. K., & Yeung, K. W. Precisely controlled delivery of magnesium ions thru sponge-like monodisperse PLGA/nano-MgO-alginate core-shell microsphere device to enable in-situ bone regeneration., *Biomaterials*., **2018**, *174*, 1-16.
28. Singh, R.; Janakiraman, S.; Agrawal, A.; Ghosh, S.; Venimadhav, A., & Biswas, K. An amorphous poly (vinylidene fluoride-co-hexafluoropropylene) based gel polymer electrolyte for magnesium ion battery., *Journal of Electroanalytical Chemistry*., **2020**, *858*, 113788.
29. Nithya, R.; Rajendran, S.; Raghu, S., & Ulaganathan, M. Li-ion conduction on nanofiller incorporated PVdF-co-HFP based composite polymer blend electrolytes for flexible battery applications., **2012**.